Desalination and Water Treatment
www.deswater.com

doi: 10.5004/dwt.2019.24457

163 (2019) 48–56
September

Effect of mixed liquor suspended solid concentration on nitrous oxide emission from an anoxic/oxic sequencing bioreactor

Xu Yan[a,*], Dongli Guo[a], Dezhi Qiu[a], Shikan Zheng[a], Mengke Jia[a], Mengjiao Zhang[a], Jingjing Liu[b], Xianfa Su[a], Jianhui Sun[a]

[a]*School of Environment, Key Laboratory for Yellow River and Huai River Water Environment and Pollution Control, Ministry of Education, Henan Key Laboratory for Environmental Pollution Control, Henan Normal University, Xinxiang 453007, Henan, China, Tel./Fax: 86-373-3325971; emails: yanxu@htu.cn (X. Yan), gdl2025@126.com (D. Guo), dezhiqiu@126.com (D. Qiu), 635744929@qq.com (S. Zheng), 27681604@qq.com (M. Jia), zhangmj112@126.com (M. Zhang), xfsu800@163.com (X. Su), sunjhhj001@163.com (J. Sun)*

[b]*School of Energy and Machinery Engineering, Jiangxi University of Science and Technology, Nanchang 310013, Jiangxi, China, Tel./Fax: 86-373-3325971; email: 339843666@qq.com*

Received 28 December 2018; Accepted 24 May 2019

ABSTRACT

Generation of nitrous oxide (N_2O), which is a strong greenhouse gas, during the biological nitrogen removal process in wastewater treatment plants has attracted widespread attention in recent years. However, the effect of mixed liquor suspended solid (MLSS) concentration on N_2O generation is poorly understood. We analyzed the N_2O emissions from three parallel anoxic/oxic biological nitrogen removal treatment systems in which the initial MLSS concentrations were 2,000 ± 100, 3,000 ± 100, and 4,000 ± 100 mg/L and the activated sludge loads were identical. The activated sludge properties and microbial community characteristics were also studied. It was found that as the initial MLSS concentration increased, the chemical oxygen demand (COD) as well as the total nitrogen, and total phosphorus removal efficiencies increased, while the nitrification rate decreased. N_2O–N conversion rates of 2.7%, 3.5%, and 4.1% corresponded to systems whose initial MLSS concentrations were 2,000 ± 100, 3,000 ± 100, and 4,000 ± 100 mg/L, respectively. The polyhydroxyalkanoate (PHA) and extracellular polymeric substance contents in the activated sludge were positively correlated with the initial MLSS concentration. The particle size distribution of the activated sludge flocs (ASFs) also varied under different MLSS concentrations; the proportion of large ASFs increased slightly as the initial MLSS concentration increased. High-throughput sequencing results showed that the bacterial species richness and microbial population diversity were enhanced as the initial MLSS concentration was increased. The relative abundance of the ammonia-oxidizing bacteria *Nitrosomonas and Sphingomonas* decreased while the total relative abundance of the denitrification bacteria with *Caldilinea*, *Ignavibacterium*, *Solitalea*, *Steroidobacter*, *Thauera*, *Comamonas*, *Lysobacter*, and *Rhodobacter* increased as the initial MLSS concentration increased.

Keywords: Wastewater treatment; Nitrous oxide; Mixed liquor suspended solid; Activated sludge properties; Microbial community characteristics

1. Introduction

The purpose of wastewater treatment plants (WWTPs) is to sanitize and purify municipal sewage. However, nitrous oxide (N_2O), a strong greenhouse gas that has a 265-fold greater greenhouse effect than carbon dioxide (CO_2), can be produced during the biological nitrogen removal (BNR) process [1]. At present, 2.8% of the anthropogenic N_2O in the

* Corresponding author.

atmosphere is generated by wastewater treatment processes, and an increase in global N_2O emissions from WWTPs of 13% is expected [2]. N_2O is an ozone-depleting compound that has been released in large quantities in recent decades and has a long steady-state lifetime of 114 years [3]. Thus, efforts to understand N_2O generation mechanisms and to establish an effective N_2O-reducing approach to wastewater treatment are essential.

Conventional BNR processes in WWTPs are composed of nitrification and denitrification processes, both of which can produce N_2O during biochemical reactions, as shown in Eqs. (1) and (2), respectively [4]. AMO and HAO are ammonia monooxygenase and hydroxylamine oxidoreductase, respectively. Nir, Nor, and Nar are nitrite reductase, nitric oxide reductase, and N_2O reductase, respectively. During the biological nitrification process (Eq. (1)), hydroxylamine (NH_2OH) oxidation, nitrifier denitrification, and heterotrophic denitrification are considered the principal pathways leading to N_2O emission [5]. In the heterotrophic denitrification process, as shown in Eq. (2), N_2O is an inevitable intermediate product. The accumulation of N_2O commonly occurs at the N_2O reduction stage when this process is disturbed or stopped.

$$NH_4^+ \xrightarrow{AMO} NH_2OH \xrightarrow{HAO} NO_2^- \xrightarrow{Nir} NO \xrightarrow{Nor} N_2O \quad (1)$$

$$NO_3^- \xrightarrow{Nar} NO_2^- \xrightarrow{Nir} NO \xrightarrow{Nor} N_2O \xrightarrow{Nos} N_2 \quad (2)$$

Numerous studies have focused on the amount and influencing factors of N_2O generation in both full-scale and lab-scale treatment processes. Kampschreur et al. [6] found large variations in N_2O emission factors, namely, 0%–95% of the influent N for the lab-scale process and 0%–14.6% of the influent N for the full-scale process. A large variation in N_2O emission factors was observed for treatment processes of similar scale [6], which indicates that the operational parameters had an influence on N_2O generation. Generally, high nitrite nitrogen (NO_2^-–N) and low dissolved oxygen (DO) concentrations are the direct indication of high N_2O emissions. In addition, the operational parameters of high pH [7], high internal recycle ratio [8], short sludge retention time (SRT) [9], and low temperature [10] are also beneficial for N_2O generation.

The mixed liquor suspended solid (MLSS) concentration is a parameter that significantly impacts oxygen transfer and nitrification and denitrification rates associated with the treatment process. The parameter also impacts the viscosity of the activated sludge and the extracellular polymeric substance (EPS) concentration [11]. An appropriate MLSS concentration can improve the removal of pollutants and decrease operating costs [12]. Song et al. [13] found that a lower MLSS concentration and shorter hydraulic retention time (HRT) led to higher nitration and N_2O emission rates in full-scale plug-flow activated sludge systems. Thus, it was hypothesized that a close relationship existed between the MLSS concentration and N_2O generation in activated sludge processes. However, the effect of MLSS concentration on N_2O emission in BNR processes has seldom been reported in previous research.

In this study, to research the effect of activated sludge concentration on N_2O generation, three parallel anoxic/oxic BNR processes with identical sludge loading were acclimated under different MLSS concentrations of 2,000 ± 100, 3,000 ± 100, and 4,000 ± 100 mg/L. The nitrification rate of the processes and the particle size distributions of the activated sludge as well as the polyhydroxyalkanoate (PHA) (including polyhydroxybutyrate [PHB], polyhydroxyvalerate [PHV]) and EPS concentrations in the three treatment systems were investigated to analyze the relationship between the sludge properties and N_2O generation. The characterization of the microbial community in the activated sludge was evaluated using high-throughput sequencing techniques.

2. Materials and methods

2.1. System description and operation

Three 2.7 L (2.4 L effective volume) sequencing batch reactor (SBR) treatment systems were set up with initial MLSS concentrations of 2,000 ± 100 (S1), 3,000 ± 100 (S2), and 4,000 ± 100 mg/L (S3). The MLSS concentrations were maintained by adjusting the rate of discharge of the excess sludge. In Fig. 1, a schematic diagram shows the laboratory SBR system. The HRT and SRT were 18 h and 12–16 d, respectively. Each cycle of the reactors was 9 h: 10 min for feeding (1.2 L wastewater), 120 min for anoxic stirring, 360 min for aeration, 40 min for settling, and 10 min for effluent withdrawal (1.2 L of treated wastewater). The DO during the aerobic phase was maintained at 2.0 ± 0.2 mg/L. To achieve anoxic conditions, N_2 was sprayed into the reactors during the anoxic phase. The three SBR treatment systems were operated at 24°C ± 2°C. The seed activated sludge was obtained from the aerobic treatment area of the Xiaoshang zhuang WWTP (Xinxiang, China). The influent wastewater was obtained from a residential area in Henan Normal

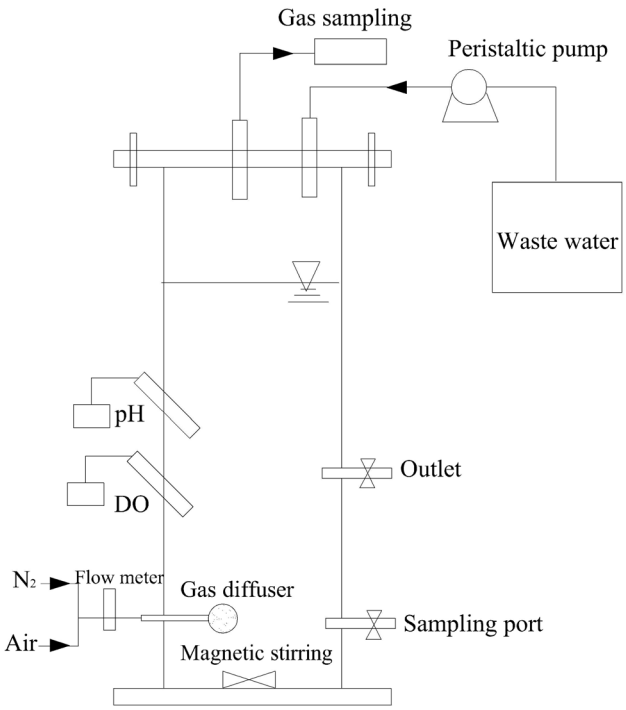

Fig. 1. Schematic of the lab-scale reactor.

University, and the wastewater qualities are listed in Table 1. To ensure identical sludge loading for each SBR, the influent wastewater for S1 and S2 was diluted with tap water. Gas and liquid samples were taken at intervals of 30 min, and sludge samples were taken once every hour.

2.2. Analytical methods

2.2.1. Gas samples

N_2O concentrations were analyzed using a gas chromatograph (Agilent 7890B, USA) with an electron capture detector. The N_2O emission rate was calculated according to the method described previously [14], and the equation used is as follows:

$$W_{N_2O} = \frac{Q \times P \times c_{N_2O} \times M_{N_2O}}{\left(R \times T \times V_L \times \text{MLVSS}\right)} \quad (3)$$

where W_{N_2O} is the emission rate of N_2O (mg/(min g MLVSS)); Q is the volumetric flow rate of gas (L/min); P is the atmospheric pressure (1 atm); c_{N_2O} is the sample gas concentration (ppm); M_{N_2O} is the molecular weight of N_2O (44.02 g/mol); R is the gas constant (0.082 L atm/(K mol)); T is the temperature (K); V_L is the volume of the bioreactor (L); and MLVSS is the mixed liquor volatile suspended solid concentration in the reactor (g/L).

The total amount of N_2O emitted in a reaction cycle was calculated by the following equation:

$$M_{N_2O} = \sum_{2}^{n}\left[\frac{1}{2}\left(W_{N_2O,n-1} + W_{N_2O,n}\right) \times \Delta t \times V_L \times \text{MLVSS}\right] \quad (4)$$

where M_{N_2O} is the N_2O emission quantity in the reaction cycle (mg); n is the number of sampling points; W_{N_2O} is the N_2O emission rate at the sampling point; Δt is the time interval between each sampling point (30 min); V_L is the volume of the bioreactor (L); and MLVSS is the mixed liquor volatile suspended solid concentration in the reactor (g/L).

2.2.2. Liquid samples

The analyses of COD, NH_4^+–N, NO_2^-–N, NO_3^-–N, TP, TN, MLSS, and MLVSS were conducted using standard methods [15]. The pH in the reactors was measured using a WTW3110 pH meter (WTW, Germany), and DO in the reactors was detected using a WTW 340i DO meter (WTW, Germany).

Table 1
Pollutants concentrations in influent wastewater

Contaminants	S1	S2	S3
COD (mg/L)	197.2 ± 21	277.4 ± 31	376.5 ± 37
NH_4^+–N (mg/L)	33.6 ± 8.6	45.1 ± 10.1	59.2 ± 13.3
NO_3^-–N (mg/L)	2.0 ± 0.6	2.9 ± 0.8	3.8 ± 1.1
NO_2^-–N (mg/L)	0.8 ± 0.3	1.1 ± 0.5	1.5 ± 0.8
TN (mg/L)	36.4 ± 2.4	50.2 ± 3.3	64.5 ± 4.1
TP (mg/L)	4.4 ± 0.7	5.9 ± 0.9	8.1 ± 1.2

The calculation of the nitrification rate was conducted using the following equation:

$$R_n = \frac{\left(\left[\text{NH}_4^+ - \text{N}\right]_{\text{anoxic}} - \left[\text{NH}_4^+ - \text{N}\right]_{\text{oxic}}\right)}{\text{MLVSS} \times t} \quad (5)$$

where R_n is the nitrification rate in the oxic phase (mg/(min g MLVSS)); $[NH_4^+–N]_{anoxic}$ is the NH_4^+–N concentration at the end of the anoxic phase (mg/L); $[NH_4^+–N]_{oxic}$ is the NH_4^+–N concentration at the end of the nitrification process (0 mg/L for the three systems); MLVSS is the mixed liquor volatile suspended solid concentration in the reactor (g/L); and t is the amount of time for the complete degradation of NH_4^+–N (min) (S1: 180 min; S2: 210 min; S3: 240 min).

2.2.3. Activated sludge samples

The particle size of the activated sludge was analyzed using a laser particle sizer (S3500, USA). The surface morphological structure of the activated sludge was analyzed by a scanning electron microscope (SEM) (JOEL JSM-6390LV, Japan). PHA, including PHB and PHV, were measured using gas chromatography [16]. Sludge mixed liquid (30–40 mL) samples from each reactor were combined with approximately 1% volume of formaldehyde to inhibit microbial activity in the sludge. Subsequently, the samples were centrifuged and the supernatant was discarded. Next, all three samples were lyophilized in a vacuum freeze dryer (FD-1A-80, Shanghai, China) operated at –56°C and 0.1 mbar for 24 h. Approximately 80 mg of freeze-dried biomass and poly (3HB-co-3HV) (CAS80181-31-3, Sigma-Aldrich Inc., USA) standards were added to 2 mL of chloroform and 2 mL of an acidified methanol solution (containing 3% sulfuric acid and 100 mg/L of sodium benzoate used as an internal standard). Subsequently, the samples and standards were digested in screw-topped glass tubes for 6 h at 100°C. After cooling, 1 mL of Milli-Q water was added, and each sample was mixed vigorously (5–10 min). After 1 h of settling, phase separation was achieved. Approximately 1 mL of the bottom organic layer was dried using granular sodium sulfate pellets (0.5–1 g) and then transferred for analysis via gas chromatography.

EPSs were extracted via the formaldehyde and sodium hydroxide method, as described previously [17]. First, a sludge sample (30–40 mL) was centrifuged (2,000 × g) for 20 min, and then the sludge pellets were resuspended to the original volume. Formaldehyde was then added at a ratio of 0.6% per sludge sample volume and mixed for 1 h. After 1 h, NaOH (1 mol/L) was introduced for 3 h. Next, ultrasonication was performed at 50 W for 2.5 min. After that, the sample was centrifuged (20,000 × g) for 20 min, and the supernatants were filtered with a membrane (0.2 μm) to collect the EPSs. In the EPSs, the protein (PN) and polysaccharides (PS) contents were measured using the Lowry method (bovine serum albumin as the standard) and the phenol–sulfuric acid method (glucose as the standard), respectively [18].

2.3. Microbial community analysis

The total genomic DNA was extracted using a PowerSoil DNA isolation kit (Mo Bio, USA). After the extraction, the quality of the DNA was examined via 1% (w/v) agarose

gel electrophoresis and then stored at –20°C for subsequent use as a template in polymerase chain reaction (PCR) amplifications.

The PCR was conducted using a Gene AmpR PCR system (9700, AB, USA) at a final volume of 60 μL using the bacterial universal primers 341F (5′-CCTACACGACGCTCTT CCGATCTN-3′) and 805R (5′-GACTGGAGTTCCTTGGCA CCCGAGAATTCCA-3′). The PCR program involved heating at 94°C for 5 min, 31 cycles of three steps (94°C for 30 s, 52°C for 30 s, 72°C for 45 s), and heating at 72°C for 10 min. A QIAquick Gel Extraction Kit (Qiagen, Chatsworth, CA, USA) was used to pool and purify replicate PCRs for each sample. The samples were sequenced on an Illumina MiSeq platform according to standard protocols.

The analysis of the microbial community composition and diversity was conducted according to the methods of a previous study [19].

3. Results and discussion

3.1. Pollutant removal performance and N_2O emission characteristics

After about 80 d of continuous operation, a stable nitrogen and COD removal efficiency was achieved. Fig. 2 shows the typical profile of the contaminants (COD, NH_4^+–N, NO_3^-–N, NO_2^-–N, TN, and TP) and N_2O emissions during the whole cycle for S1, S2, and S3. Fig. 3 shows the concentration

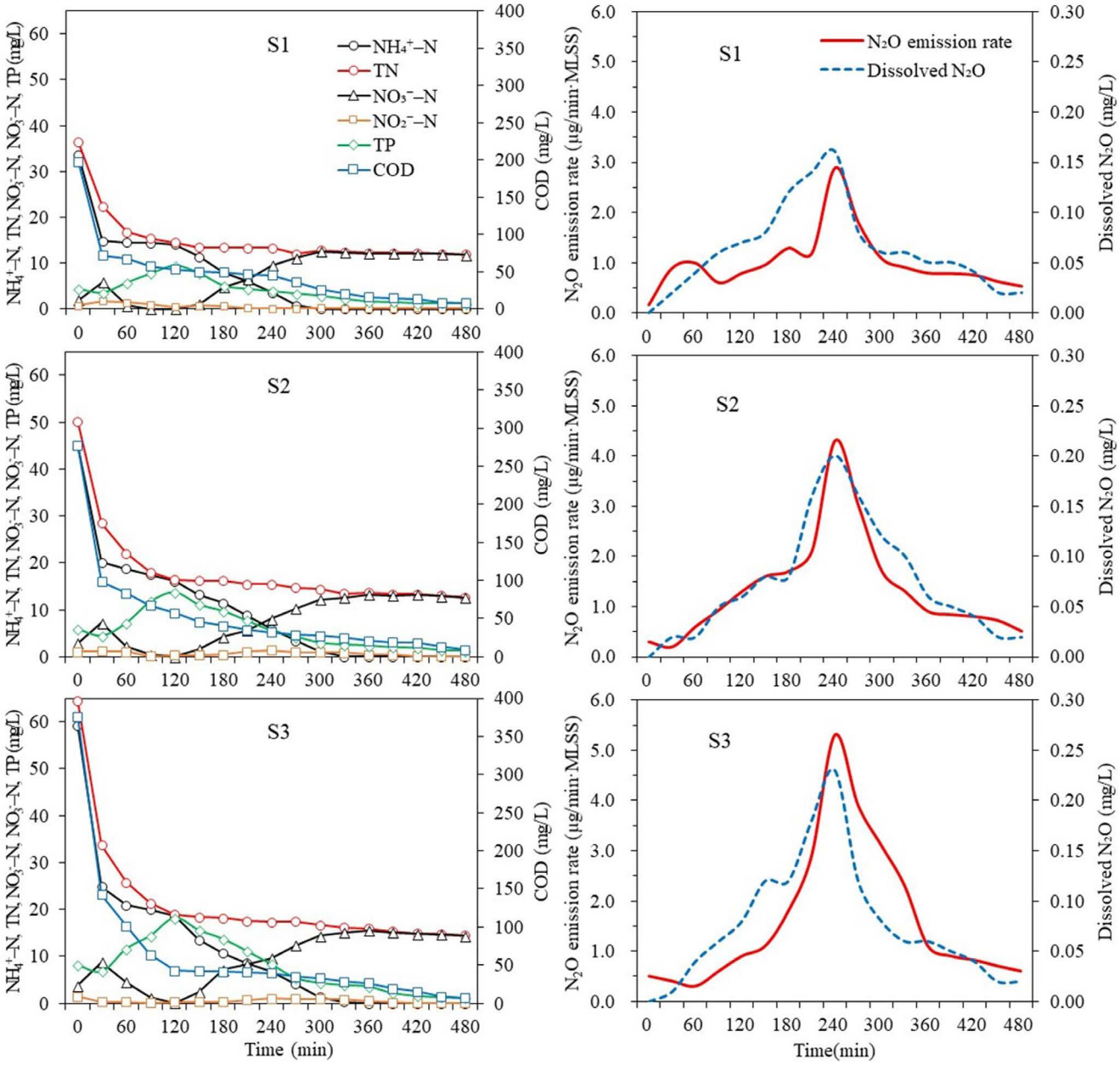

Fig. 2. Time profiles of NH_4^+–N, COD, NO_2^-–N, NO_3^-–N, TN, and TP concentrations as well as N_2O emission rates for S1, S2, and S3.

variation characteristics of PHA (PHB and PHV) during the reaction period. The N_2O emissions and nitrification rates are listed in Table 2.

The activated sludge concentration had a significant influence on the removal of pollutants. When the MLSS concentration increased from 2,000 ± 100 to 4,000 ± 100 mg/L, the COD removal efficiency increased from 95.9% to 98.2%, while the nitrification rate decreased from 5.2×10^{-2} to 2.3×10^{-2} mg/(min g MLVSS) (Table 2). The TN removal efficiencies also varied among the systems and were 67.3%, 74.7%, and 77.5% for S1, S2, and S3, respectively. In this process, a large proportion of the removed NH_4^+–N was converted to NO_3^-–N, which was retained in the effluent (Fig. 3). The TP removal efficiency was also positively correlated with the activated sludge concentration, increasing from 70.5% to 86.4% with the increase in MLSS concentration.

As the MLSS concentration increased, the N_2O production and conversion rates significantly increased (Table 2). The N_2O generation in S3 was about 3.1 times higher than it was in S1. The N_2O emission trend was similar among the three SBRs; the N_2O emission rates during the aerobic process were higher than those during the anoxic process, and the peaks appeared at 240 min for all parallels. This phenomenon indicated that N_2O was primarily generated during the aerobic process. During this process, low DO and high ammonia concentrations were found to significantly enhance N_2O production [6]. It is noted that a high activated sludge concentration benefited the removal of pollutants but simultaneously promoted N_2O generation in this treatment system.

PHA is an intracellular storage compound that with two monomers of PHB and PHV, which are highly correlated with N_2O generation [20]. Typically, PHA is synthesized during the anoxic process as a carbon source, and is consumed during the phosphate accumulation, aerobic denitrification, and cell maintenance phases of the aerobic process [7]. In this study, the MLSS concentration influenced the composition of PHA; at the end of the anoxic phase, the PHA concentrations were 4.8, 6.4, and 7.7 mg/g MLSS for S1, S2, and S3, respectively. With the increase in MLSS concentration, the amounts of synthesized PHA and N_2O emissions increased simultaneously. During the aerobic process, the decreases in the concentrations of TP and TN were 8.2 and 2.6 mg/L, 12.5 and 3.7 mg/L, and 17.1 and 4.4 mg/L for S1, S2, and S3, respectively, which indicated that phosphate accumulation and aerobic denitrification both occurred and that PHA was degraded as an electron donor in this phase. Some studies found that N_2O emission was enhanced during denitrification when PHA was used as a carbon source [21].

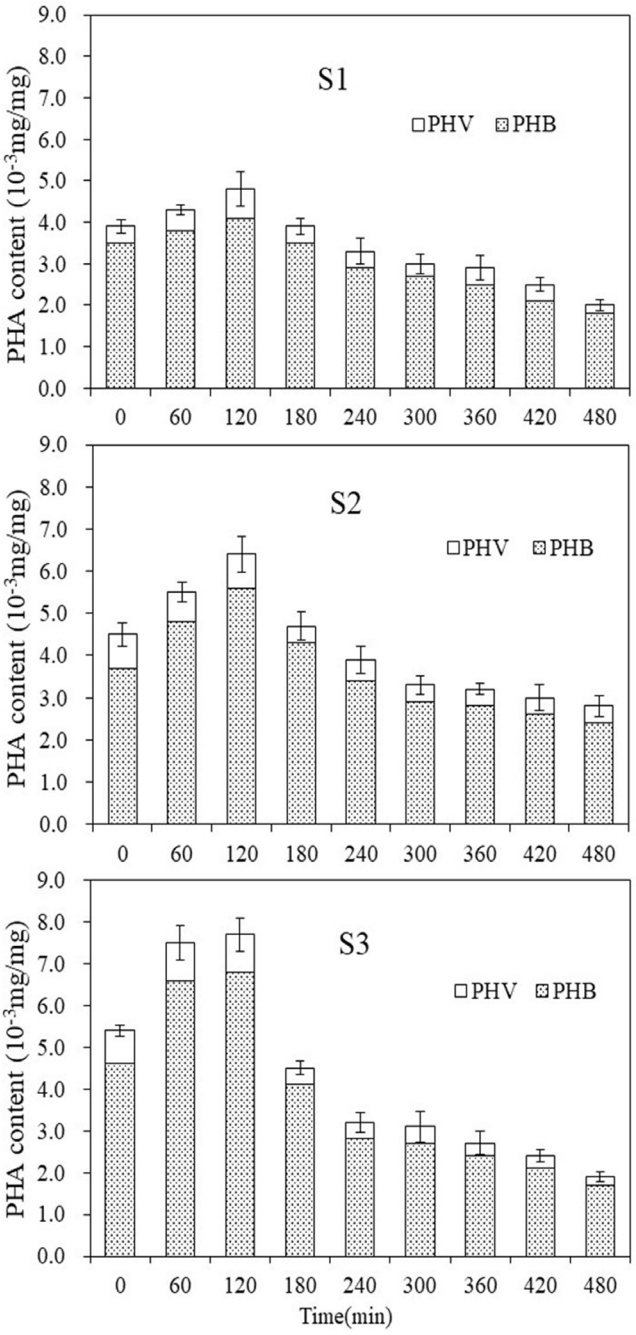

Fig. 3. Time profiles of PHA (including PHB and PHV) content during the reaction period for S1, S2, and S3.

Table 2
N_2O generation situation and nitrification rate in S1, S2, and S3

MLSS (mg/L)	N_2O average emission rate (μg/min g MLVSS)	Nitrification rate (mg NH_4^+–N/min g MLVSS)	Total N_2O generation (mg)	N_2O–N conversion rate (%)
S1	1.3	5.2×10^{-2}	2.5	2.7
S2	1.7	3.5×10^{-2}	4.9	3.5
S3	2.1	2.5×10^{-2}	7.7	4.1

N_2O–N conversion rate = (total N_2O–N emission)/(total nitrogen removed) × 100%.

This is a potential reason for the observed positive correlation between N_2O emission and PHA concentration in this study.

3.2. Sludge characteristics analysis

The concentration of activated sludge showed a significant influence on sludge characteristics. Fig. 4 shows the particle size distributions of the activated sludge flocs (ASFs) in S1, S2, and S3. The SEM images of activated sludge in the systems are shown in Fig. 5. The contents of PS and PN under different MLSS concentrations are exhibited in Fig. 6.

Normal distributions of ASF sizes were observed in the three SBRs, and the majority of the ASFs were in the range of 0–150 μm. As the MLSS concentration increased, the proportion of the larger ASFs was elevated slightly (Fig. 4). The morphology of the activated sludge (Fig. 5) also indicated the particle size of the sludge flocs increased with increasing MLSS. EPS plays an important role in bacterial agglutination and in the formation of ASFs, which are primarily composed of PS and PN. In this study, the PS and PN contents and MLSS concentration showed a positive correlation.

ASFs play a fundamental role in the wastewater treatment process. They are formed by aggregates of microorganisms, suspended solids, and extracellular polymers. The microscopic mass transfer efficiency of ASFs is closely related to the pollutant removal efficiency. Han et al. [22] reported that the DO concentrations in the inner ASFs were lower than those at the surface, and the DO distributions depended on the grain diameter of the flocs. With an increase in floc grain diameter from 100 to 250 μm, the DO concentrations in the floc centers decreased from 10% to 55%, respectively. In a one-stage autotrophic nitrogen removal system, Wang et al. [23] observed that the DO and N_2O concentrations were closely related to the depth of the biofilm. As the depth of the biofilm increased, the DO concentration sharply decreased, while the N_2O concentration increased. Higher MLSS concentration in an activated sludge system led to a sharper depletion in the DO concentration in flocs [24]. This was likely due to the competition for DO between microorganisms being promoted, which resulted in an enhanced limitation of oxygen transport in ASFs. Even in the aerobic phase, an anoxic environmental condition could be formed at the inner area of the ASFs, which would promote the denitrification reactions and N_2O generation [6].

The EPS content is another factor that limits the oxygen mass transport for ASFs. In the activated sludge wastewater

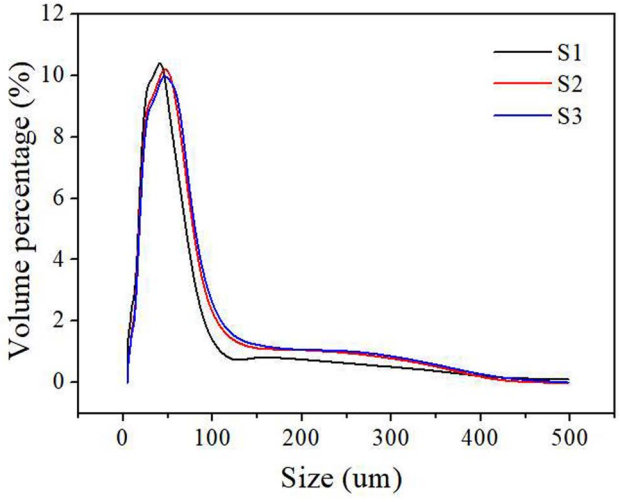

Fig. 4. Particle size distribution of the ASFs under different MLSS concentrations.

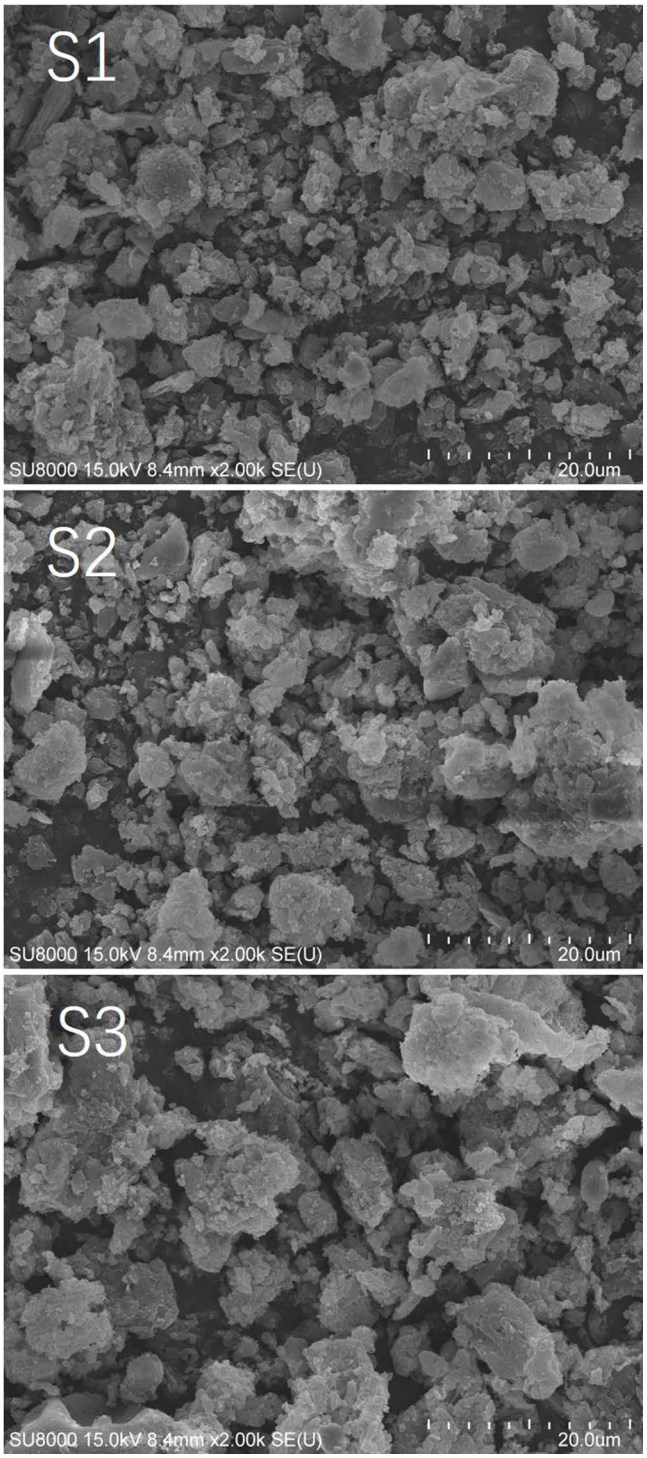

Fig. 5. SEM images of activated sludge for S1, S2 and S3.

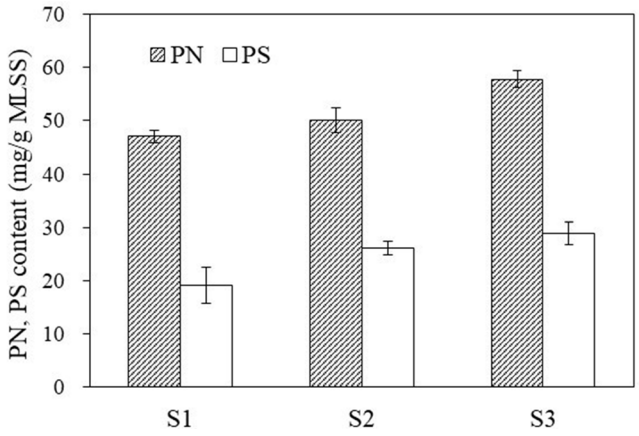

Fig. 6. Polysaccharide and protein concentrations in S1, S2, and S3.

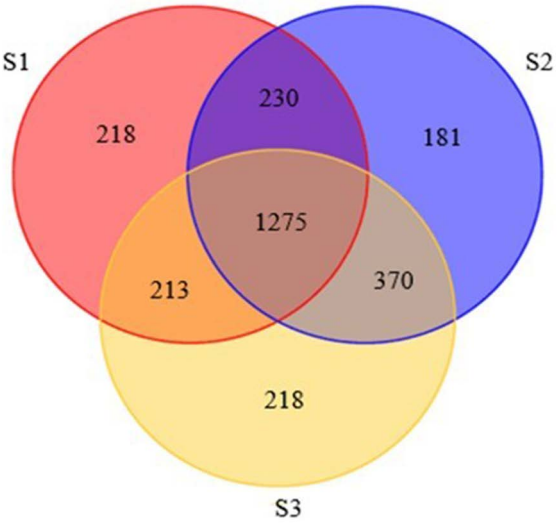

Fig. 7. Venn diagram of the OTUs distribution in S1, S2, and S3.

treatment process, EPSs cover the surface or fill the interior of cells in microbial aggregates, which significantly influences the effective diffusion coefficient of substrates. A high EPS content is disadvantageous for mass transfer. In the flocs, a high concentration of organic matter can enhance the DO consumption rate, increase microorganism growth and EPS content, and decrease the mass transfer rate [25]. In a continuous stirred-tank process, with the EPS per unit sludge increased, Fan et al. [24] observed a more extensive anoxic zone and lower DO transfer capability in ASFs using microelectrode technology. In this study, the influent organic concentration was increased with increasing MLSS concentration to maintain identical sludge loading.

3.3. Microbiological community characteristics

To investigate the microorganism characteristics under different MLSS concentrations, a high-throughput sequencing analysis using 16S rRNA amplicons technology was employed in this study. Fig. 7 shows a Venn diagram of the operational taxonomic units (OTUs) distribution in the systems. The microbial diversity parameters and the relative abundances (more than 0.5%) of the bacterial community groups at the phylum and genus level in the three systems are shown in Table 3 and Fig. 8.

The results implied that varying MLSS concentrations developed distinct microbial communities in the activated sludge. The variation in microbial community composition was observed by an analysis of the number of OTUs (Fig. 7). The OTUs were 1,936; 2,056; and 2,076 for S1, S2, and S3, respectively. Because identical seed sludge was processed at the beginning of the operation, 1,275 identical OTUs were observed. In addition, the PD whole tree, Chao1, Shannon index, and Simpson index microbial diversity parameters showed a positive correlation with the MLSS concentration. This indicated that the bacterial species richness and microbial population diversity increased with the increase in MLSS concentration in the SBRs.

The phylogenetic structure of the bacterial communities in S1, S2, and S3 was characterized at the phylum and genus levels (Fig. 8). The bacterial community compositions were distinct, and the relative abundances of the dominant species varied with the increase in MLSS concentration. At the phylum level, the relative abundances of Bacteroidetes and Acidobacteria showed a negative correlation with the MLSS concentration, whereas the relative abundances of Verrucomicrobia, Planctomycetes, Firmicutes, and Actinobacteria showed a positive correlation with the MLSS concentration. The relative abundances of the dominant genera *Blastocatella* and *Ferruginibacter* decreased from 22.0% to 11.1% and from 17.3% to 3.1% following the increase in MLSS concentration from 2,000 ± 100 to 4,000 ± 100 mg/L, respectively, while the relative abundances of the genus *Haliscomenobacter* increased from 2.3% to 11.2%.

Some *Blastocatella* species are aerobic and are ammonia-oxidizing bacteria (AOB) that can generate N_2O through autotrophic denitrification during aerobic treatment processes [26]. The relative abundances of AOB *Nitrosomonas* and *Sphingomonas* decreased from 1.1% to 0.5% and from 0.07% to 0.06%, respectively, with the increase in MLSS. The relative abundances of NOB *Nitrospira* were 0.11%, 0.10%, and 0.07% for S1, S2, and S3, respectively. This was the primary case for the decrement of nitrification rate as the MLSS increased. All known species belonging to the genus *Ferruginibacter* are strictly aerobic, and some members, such as *Ferruginibacter alkalilentus* and *Ferruginibacter lapsinanis*, are capable of hydrolyzing organic matter [27]. *Haliscomenobacter* is a filamentous microorganism belonging to Bacteroidetes; it is negatively correlated with DO and is commonly present in activated sludge from both municipal

Table 3
Microbial diversity parameters in S1, S2, and S3

Sample	PD whole tree	Chao1	Shannon	Simpson
S1	157	2,422	6.3	9.2×10^{-1}
S2	163	2,493	6.9	9.6×10^{-1}
S3	162	2,532	7.2	9.7×10^{-1}

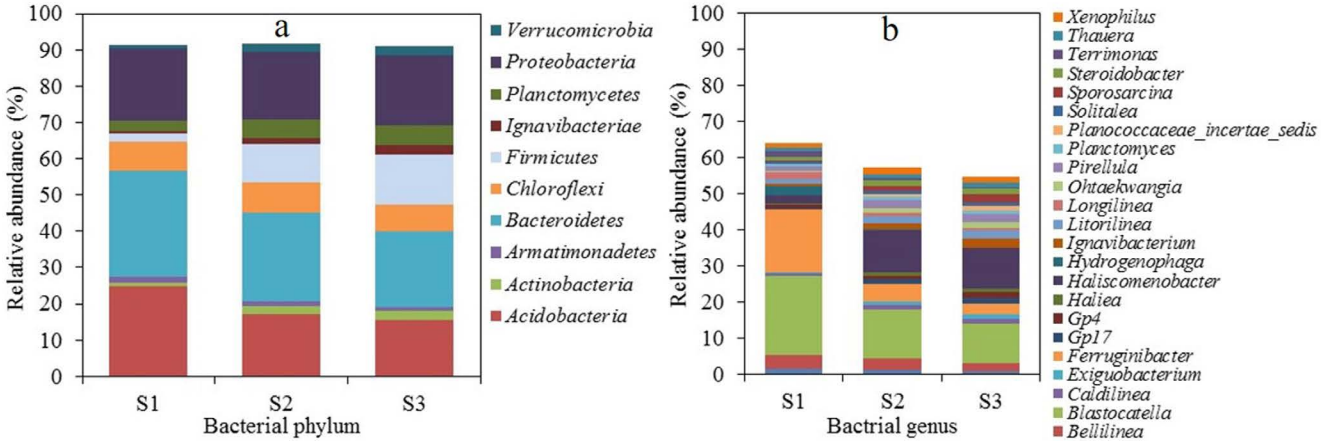

Fig. 8. Relative abundances of major bacterial groups at (a) phylum and (b) genus levels in S1, S2, and S3 (relative abundance >1%).

and industrial WWTPs [28]. Numerous groups responsible for denitrification process were detected in the systems, including the following dominant ones, with relative abundances >0.5%; *Caldilinea* (0.67%, 1.37%, 1.16%), *Ignavibacterium* (0.77%, 1.63%, 2.68%), *Solitalea* (0.46%, 1.01%, 0.92%), *Steroidobacter* (1.08%, 1.73%, 1.70%), *Thauera* (0.83%, 1.08%, 1.13%), *Comamonas* (0.79%, 0.58%, 0.54%), *Lysobacter* (0.27%, 0.55%, 0.73%), and *Rhodobacter* (0.29%, 0.40%, 0.63%) [29,30]. The total relative abundances of denitrifying bacteria were 6.34%, 9.50%, and 10.85% for S1, S2, and S3, respectively. These results showed that the increase in the MLSS concentration led to an overall increase in the relative abundance of denitrifying bacteria. This was probably the reason for the highest denitrification rate that was observed in S3.

Considering the oxygen requirements of *Blastocatella*, *Ferruginibacter*, *Haliscomenobacter*, and denitrification bacteria, their relative abundances in the SBRs were probably related to the DO variation in the microenvironment of the ASFs caused by the increased sludge pollutant concentrations. Thus, the increase in N_2O generation associated with the increase in the MLSS concentration was primarily caused by heterotrophic denitrification.

In WWTPs, the microbial community structure plays an important role in the removal of pollutants, and it is impacted by influent composition, operational parameters, and environmental conditions [31]. Generally, the microbial diversity reflects the stability of the biochemical treatment system and the complex and multi-stage process units or systems that lead to higher microbial diversity [32]. The microenvironment of the ASFs also influenced the bacterial population distribution in ASFs, which was closely related to the aforementioned driving factors [22,24]. The microbial structure, composition, and distribution responded to the microenvironment variation in ASFs with different grain diameters [22]. In this study, with the increased activated sludge concentration, the competition for substrate between microorganisms and mass transport resistance in the flocs was enhanced, which led to more complex environmental conditions. Consequently, the bacterial species richness, microbial population diversity, and relative abundance of anaerobes were all positively correlated with the increase in the MLSS concentration.

4. Conclusion

In the BNR process, MLSS concentration played an important role in the treatment effect and N_2O emission. When the MLSS concentration increased from 2,000 ± 100 to 4,000 ± 100 mg/L, the N_2O–N conversion rate increased from 2.7% to 4.1%. The PHA contents, EPS contents, and ratio of larger flocs in the activated sludge were positively correlated with the MLSS concentration. High-throughput sequencing showed that bacterial species richness and microbial population diversity were enhanced with an increase in the MLSS concentration. The relative abundances of AOB decreased, and the relative abundances of denitrification bacteria increased with the enhanced MLSS concentration, indicating that N_2O generation from heterotrophic denitrification was promoted.

Acknowledgements

This research was financially supported by the National Natural Science Foundation of China (No. 51408199), the Natural Science Foundation of Henan Province of China (No. 182300410157) and the Jiangxi Provincial Department of Science and Technology (No. 20142BAB213026).

References

[1] IPCC, Climate Change 2014: Synthesis Report, IPCC, Switzerland, 2014.
[2] Y. Law, L. Ye, Y. Pan, Z. Yuan, Nitrous oxide emissions from wastewater treatment processes, Philos. Trans. R. Soc. London, Ser. B, 367 (2012) 1265–1277.
[3] A.R. Ravishankara, J.S. Daniel, R.W. Portmann, Nitrous oxide (N_2O): the dominant ozone-depleting substance emitted in the 21st century, Science, 326 (2009) 123–125.
[4] S. Sun, Z. Bao, R. Li, D. Sun, H. Geng, X. Huang, J. Lin, P. Zhang, R. Ma, L. Fang, X. Zhang, X. Zhao, Reduction and prediction of N_2O emission from an anoxic/oxic wastewater treatment plant upon DO control and model simulation, Bioresour. Technol., 244 (2017) 800–809.
[5] B.-J. Ni, Z. Yuan, Recent advances in mathematical modeling of nitrous oxides emissions from wastewater treatment processes, Water Res., 87 (2015) 336–346.
[6] M.J. Kampschreur, H. Temmink, R. Kleerebezem, M.S.M. Jetten, M.C.M. van Loosdrecht, Nitrous oxide emission during wastewater treatment, Water Res., 43 (2009) 4093–4103.

[7] Z. Wang, Y. Meng, T. Fan, Y. Du, J. Tang, S. Fan, Phosphorus removal and N_2O production in anaerobic/anoxic denitrifying phosphorus removal process: long-term impact of influent phosphorus concentration, Bioresour. Technol., 179 (2015) 585–594.
[8] X. Yan, Y. Han, Q. Li, J. Sun, X. Su, Impact of internal recycle ratio on nitrous oxide generation from anaerobic/anoxic/oxic biological nitrogen removal process, Biochem. Eng. J., 106 (2016) 11–18.
[9] K. Hanaki, Z. Hong, T. Matsuo, Production of nitrous oxide gas during denitrification of wastewater, Water Sci. Technol., 26 (1992) 1027–1036.
[10] N. Adouani, L. Limousy, T. Lendormi, O. Sire, N_2O and NO emissions during wastewater denitrification step: influence of temperature on the biological process, C.R. Chim., 18 (2015) 15–22.
[11] M. Mori, I. Seyssiecq, N. Roche, Rheological measurements of sewage sludge for various solids concentrations and geometry, Process Biochem., 41 (2006) 1656–1662.
[12] S. Sun, J. Lu, Z. Guo, Z. Sheng, P. Cao, A flexible aeration strategy based on the removal of COD and MLSS in treating tomato paste wastewater, Desal. Wat. Treat., 51 (2013) 2109–2115.
[13] K. Song, T. Suenaga, A. Hamamoto, K. Satou, S. Riya, M. Hosomi, A. Terada, Abundance, transcription levels and phylogeny of bacteria capable of nitrous oxide reduction in a municipal wastewater treatment plant, J. Biosci. Bioeng., 118 (2014) 289–297.
[14] Z. Hu, J. Zhang, S. Li, H. Xie, J. Wang, T. Zhang, Y. Li, H. Zhang, Effect of aeration rate on the emission of N_2O in anoxic–aerobic sequencing batch reactors (A/O SBRs), J. Biosci. Bioeng., 109 (2010) 487–491.
[15] CEPB, Standard Methods for Examination of Water and Wastewater, 4th ed., China Environmental Science Press, Beijing, 2004.
[16] A. Oehmen, B. Keller-Lehmann, R.J. Zeng, Z.G. Yuan, J. Keller, Optimisation of poly-β-hydroxyalkanoate analysis using gas chromatography for enhanced biological phosphorus removal systems, J. Chromatogr. A, 1070 (2005) 131–136.
[17] H. Liu, H.H.P. Fang, Extraction of extracellular polymeric substances (EPS) of sludges, J. Biotechnol., 95 (2002) 249–256.
[18] F. Bo, R. Palmgren, K. Keiding, P.H. Nielsen, Extraction of extracellular polymers from activated sludge using a cation exchange resin, Water. Res., 30 (1996) 1749–1758.
[19] J. Liu, X.-x. He, X.-r. Lin, W.-c. Chen, Q.-x. Zhou, W.-s. Shu, L.-n. Huang, Ecological effects of combined pollution associated with e-waste recycling on the composition and diversity of soil microbial communities, Environ. Sci. Technol., 49 (2015) 6438–6447.
[20] Y. Liu, L. Peng, X. Chen, B.-J. Ni, Mathematical modeling of nitrous oxide production during denitrifying phosphorus removal process, Environ. Sci. Technol., 49 (2015) 8595–8601.
[21] Y. Zhou, M. Lim, S. Harjono, W.J. Ng, Nitrous oxide emission by denitrifying phosphorus removal culture using polyhydroxyalkanoates as carbon source, J. Environ. Sci., 24 (2012) 1616–1623.
[22] Y. Han, J. Liu, X. Guo, L. Li, Micro-environment characteristics and microbial communities in activated sludge flocs of different particle size, Bioresour. Technol., 124 (2012) 252–258.
[23] X.-X. Wang, F. Fang, Y.-P. Chen, J.-S. Guo, K. Li, H. Wang, N_2O micro-profiles in biofilm from a one-stage autotrophic nitrogen removal system by microelectrode, Chemosphere, 175 (2017) 482–489.
[24] H. Fan, X. Liu, H. Wang, Y. Han, L. Qi, H. Wang, Oxygen transfer dynamics and activated sludge floc structure under different sludge retention times at low dissolved oxygen concentrations, Chemosphere, 169 (2017) 586–595.
[25] X.-H. Zhou, H.-C. Shi, Q. Cai, M. He, Y.-X. Wu, Function of self-forming dynamic membrane and biokinetic parameters' determination by microelectrode, Water Res., 42 (2008) 2369–2376.
[26] Z. Jin, X. Xie, J. Zhou, K. Bei, Y. Zhang, X. Huang, M. Zhao, H. Kong, X. Zheng, Blackwater treatment using vertical greening: efficiency and microbial community structure, Bioresour. Technol., 249 (2018) 175–181.
[27] J.H. Lim, S.H. Baek, S.T. Lee, *Ferruginibacter alkalilentus* gen. nov., sp. nov. and *Ferruginibacter lapsinanis* sp. nov., novel members of the family 'Chitinophagaceae' in the phylum Bacteroidetes, isolated from freshwater sediment, Int. J. Syst. Evol. Microbiol., 59 (2009) 2394–2399.
[28] C. Kragelund, C. Levantesi, A. Borger, K. Thelen, D. Eikelboom, V. Tandoi, Y. Kong, J. Krooneman, P. Larsen, T.R. Thomsen, P.H. Nielsen, Identity, abundance and ecophysiology of filamentous bacteria belonging to the Bacteroidetes present in activated sludge plants, Microbiology, 154 (2008) 886–894.
[29] Q.L. He, L. Chen, S.J. Zhang, R.F. Chen, H.Y. Wang, Hydrodynamic shear force shaped the microbial community and function in the aerobic granular sequencing batch reactors for low carbon to nitrogen (C/N) municipal wastewater treatment, Bioresour. Technol., 271 (2019) 48–58.
[30] J. Meng, J.L. Li, J.Z. Li, J. Nan, K.W. Deng, P. Antwi, Effect of temperature on nitrogen removal and biological mechanism in an up-flow microaerobic sludge reactor treating wastewater rich in ammonium and lack in carbon source, Chemosphere, 216 (2019) 186–194.
[31] X. Yan, J. Zheng, Y. Han, J. Liu, J. Sun, Effect of influent C/N ratio on N_2O emissions from anaerobic/anoxic/oxic biological nitrogen removal processes, Environ. Sci. Pollut. Res., 24 (2017) 23714–23724.
[32] Y. Chen, S. Lan, L. Wang, S. Dong, H. Zhou, Z. Tan, X. Li, A review: driving factors and regulation strategies of microbial community structure and dynamics in wastewater treatment systems, Chemosphere, 174 (2017) 173–182.